

# Hydrogen magnetic reaction gene regulation

Yeon Sook Kim<sup>1</sup>, Dae Gwan Lee<sup>2</sup>, Suk Keun Lee<sup>3\*</sup>

<sup>1</sup>Department of Dental Hygiene, College of Health, Cheongju University, Cheongju, Korea; <sup>2</sup>Department of Mathematical Sciences, KAIST, Daejeon, Korea; <sup>3</sup>Department of Oral Pathology, College of Dentistry, Gangneung-Wonju National University, Gangneung, Korea

**Running title: Hydrogen magnetic reaction gene regulation**

**\*Corresponding:** Suk Keun Lee, DDS, Ph.D.  
Department of Oral Pathology, College of Dentistry, Gangneung-Wonju National University, 123 Chibyun-dong, Gangneung, 210-702, Korea  
Tel : +82-33-640-2228  
Fax: +82-33-642-6410  
E-mail : [sukkeunlee@hanmail.net](mailto:sukkeunlee@hanmail.net)

# Hydrogen magnetic reaction gene regulation

## SUMMARY

A new gene regulation system using weak magnetic field can induce the hydrogen magnetic reaction (HMR) in hydrogen atoms, and subsequently affect the electrostatic polarity of hydrogen bonds in DNA base pairs. The HMR can sequentially activate the DNA base pair polarities of target DNA. With the characteristic base pair polarities of DNA duplex the (pyrimidine)<sub>m</sub>-(purine)<sub>n</sub> DNA segment is a basic unit to maintain and to accumulate the electrostatic energy of DNA duplex (1). To enhance the polarities of objective DNA this HMR gene regulation (HMR-GR) uses the polarized magnetic field with optimal nucleotide exposure time for T:A and C:G base pairs (50 msec and 80 msec, respectively). The targeting efficiency of HMR-GR to the objective DNA is theoretically up to 25%. In the present study, the HMR-GR expanded the conformation of oligo-dsDNA *in vitro*, implicating the active state of DNA, and also enhanced the restriction endonuclease digestion, *in vitro* RNA transcription, and the production of green fluorescence protein and β-galactosidase by using each RE site sequence and relevant promoter sequence, respectively. Taken together, it is assumed that the HMR-GR is an effective and safe method to control the multiple genes sequentially by activating their specific DNA motifs.

**Keywords:** Hydrogen magnetic reaction, DNA base pair polarity, Pyu DNA segment

## INTRODUCTION

There are many kinds of gene therapy methods to treat not only human diseases but also to regulate different biological organisms by using drugs, genetic materials, vectors, and physicochemical stimuli, etc. Here, we developed a strategy of HMR-GR using cyclic magnetic field to control specific base pair polarities of target DNA via hydrogen magnetic reaction in their hydrogen bonds. The general introduction for the HMR-GR is as follows.

### *Hydrogen magnetic reaction (HMR) in hydrogen bonds*

Magnetic field is known to induce electromagnetic reaction in a hydrogen atom. In this study we call the

electromagnetic reaction of hydrogen atom as the hydrogen magnetic reaction (HMR) in order to keep the effect of magnetic polarity from the variable electric field effect. While strong magnetic field, e.g., over 1 Tesla (T), may induce proton spin reaction, the weaker magnetic field such as geomagnetic field (about 50  $\mu$ T) (2-4) is also enough to induce spin-orbit interaction of electrons in hydrogen atom. Repeated HMRs with weak magnetic field can affect the associated hydrogen bonds, e.g., HO--H in water (5-7) and HN--H/NH--O in DNA base pairs (8) (Figure 1A).

The HMR-GR is a transient phenomenon occurred in a hydrogen bond, immediately related to the normal atomic status, but still able to elicit the change of electrostatic charge between the hydrogen donor and hydrogen acceptor molecules. The putative HMR energy in a hydrogen atom is ascribed to the spin-orbit interaction momentum, thereby it is calculated by the equation of Zeeman effect under weak magnetic field ( $E = g_l \mu_B B m_l$ ). Where  $g_l$  is the orbital gyromagnetic ratio,  $\mu_B$  is the Bohr magneton,  $B$  is the magnetic field strength, and  $m_l$  is the magnetic quantum number (9-11). For example, 100 Gauss of magnetic field induces about 1.2  $\mu$ eV of HMR energy in a hydrogen atom by Zeeman effect, which is depending on the direction of the magnetic field and mostly transferred into the hydrogen bond, e.g., NH--O in a DNA base pair, if the quantum radiation were negligible. In this aspect, HMR can increase the electrostatic charge of hydrogen bonding between hydrogen and oxygen, and more importantly, repetition of HMR in a certain pattern activates the DNA by accumulating the electrostatic polarities in the DNA segment. About 200 repetition of HMR may increase the spin-orbit momentum, up to approximately 240  $\mu$ eV in a hydrogen bond, which may be effective on the structural change of target DNA base pair (Figure 1).

In this study the magnetic field in the direction from oxygen to hydrogen in hydrogen bonding is called polarized magnetic field (PMF) which can increase the hydrogen bond strength (Figure 1B), while the PMF in the reverse direction is called reverse PMF which can decrease the hydrogen bond strength by reversing the direction of spin-orbit interaction (Figure 1C).

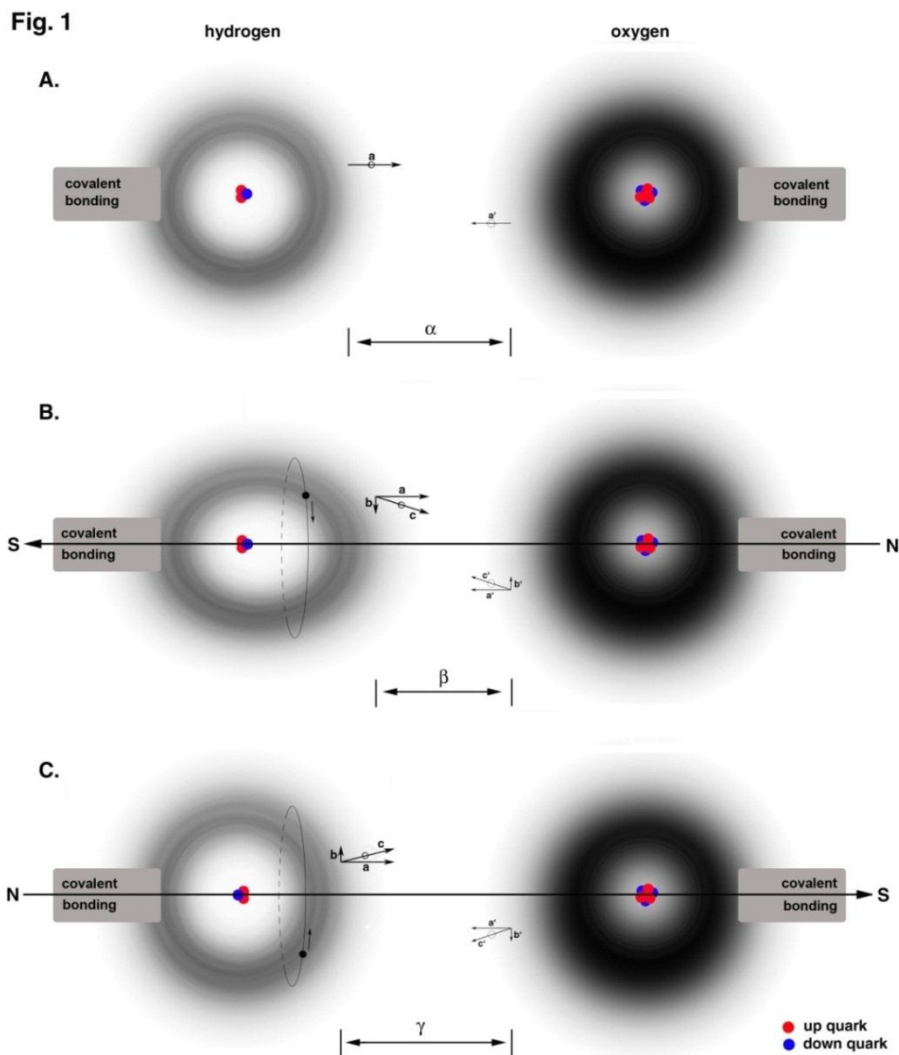


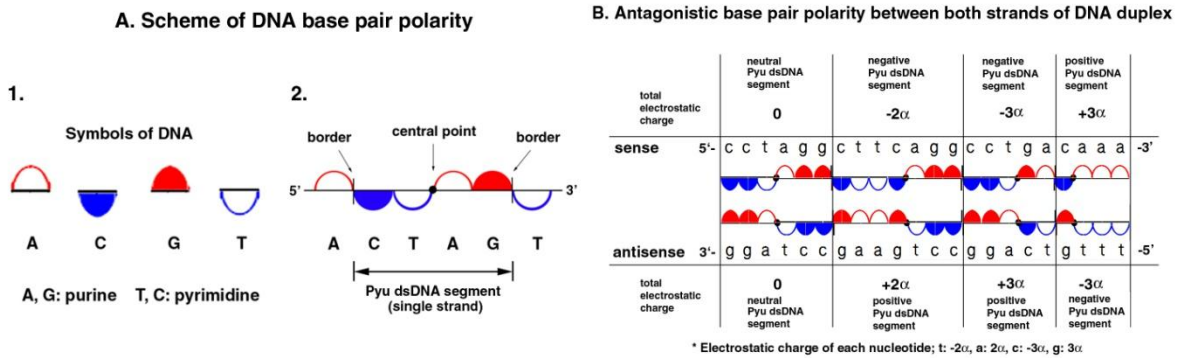
Figure 1. The hydrogen magnetic reaction (HMR) by weak magnetic field in hydrogen bonding between a hydrogen and an oxygen. (A) Hydrogen bonding without magnetic field (MF), noted the electron pairing between a hydrogen and an oxygen (arrows). (B) 100 Gauss MF parallel to the direction of hydrogen bonding induces the spin-orbit interaction, which is calculated about  $1.2 \mu\text{eV}$  in a hydrogen atom (b) but negligible in an oxygen atom ( $b'$ ). With the HMR repeated 200 times the strength of spin-orbit interaction is accumulated up to about  $240 \mu\text{eV}$ , and can change the hydrogen bond strength from about  $605 \mu\text{eV}$  (a) to about  $651 \mu\text{eV}$  (c), resulted in shorter distance ( $\beta$ ) between a hydrogen and an oxygen compared to the normal ( $\alpha$ ). This direction of MF is called the polarized magnetic field (PMF). (C) Hydrogen bonding with the reverse PMF, producing a longer distance ( $\gamma$ ) between hydrogen and oxygen than the normal ( $\alpha$ ) by reversing the direction of spin-orbit interaction in a hydrogen atom.

### *Specific patterns of DNA base pair polarities*

Due to the different electrostatic polarities between hydrogen donor and hydrogen acceptor in a hydrogen bond, pyrimidine is negative while purine is positive in a DNA base pair relatively, while C:G base pair containing three hydrogen bonds has stronger hybridization than T:A base pair containing two hydrogen bonds. For the purpose of effective visualization, genetic codes composed of A, C, G, T are symbolized based on their different electrostatic charges using the characteristic nucleotide symbols shown in Figure 2A1 (1).

Using the nucleotide symbols, different polarity groups of DNA are visible and electrostatic potentials can be calculated, so that it becomes easier to analyze the intrinsic potential of genetic information (Figure 2C). Since each strand of DNA duplex is polarized in the direction from 5' to 3', the transferred electrostatic charge from the 5'-pyrimidine can easily flow to 3'-purine charged positively, whereas it can hardly flow reversely from 3'-pyrimidine to 5'-purine. Based on this consideration, DNA sequence can be divided into DNA segments composed of (pyrimidine)<sub>m</sub>-(purine)<sub>n</sub> (m, n; natural numbers), which are to be referred as Puy DNA segments (Figure 2A2). These Puy DNA segments are the basic units of DNA duplex that can maintain and accumulate the electrostatic charge of DNA base pairs (Figure 2B). The Puy DNA segment shows stronger hybridization than Puy DNA segment ((purine)<sub>n</sub>-(pyrimidine)<sub>m</sub>), and forms a stable DNA conformation to maintain the interaction with other molecules (1,12-14). The DNA sequences for the HMR-GR were analyzed by the DNA base pair polarity program, and the characteristic Puy DNA segments were selected to target the objective DNA.

Fig. 2



**C. Every DNA code can be translated into DNA base pair polarity symbols disclosing Pylus DNA segments.**

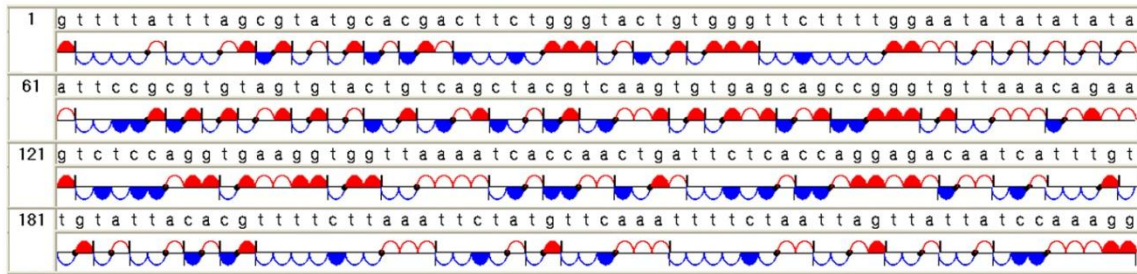


Figure 2. The symbolization of DNA sequences based on the concept of DNA base pair polarity. (A) The purines, A and G, are the upward half-round in red color, and the pyrimidines, T and C, are the downward half-round in blue color. And the half-rounds of T and A are empty, while the half-rounds of C and G are filled with blue and red color, respectively. (B) The nucleotide symbols of ACTAGT are arranged on the horizon line, and then two borders appear between purine and pyrimidine in order. A Pylus DNA segment, CTAG, is defined between the borders. The point changing from pyrimidine to purine in a Pylus DNA segment is called a central point. The both strands of Pylus DNA segment are antagonistic each other in their polarity amount as well as in their polarity directions. (C) The DNA sequences described in alphabet, A, C, G, and T are somehow monotonous, but the symbolized DNA sequences may disclose the characteristic electrostatic potentials of DNA code.

## ***Generation of cyclic magnetic field for HMR-GR***

In the HMR-GR system the electromagnetic field was generated by direct electric current between a pair of electromagnet arranged longitudinally, and its intensity was limited up to 100 Gauss in order to prevent a biohazard (15,16). The HMR-GR apparatus has 5 or 6 pairs of electromagnets arranged in circular fashion simulating the structure of DNA duplex, which has about 10.5, 11, and 12 base pairs per a cycle for B, A, Z type DNA, respectively. The pairs of electromagnets are placed in cyclic fashion heading toward the center, where the objective DNAs will be placed. The inside of HMR-GR apparatus was cooled by ventilation to keep with the room temperature.

In the DNA base pairs, the pyrimidine and purine have different electrostatic polarities, which are distinguishable by the direction of magnetic field in the HMR-GR. The magnetic field which has the same polarity of DNA base pair is called a polarized magnetic field (PMF), which directs from T to A for T:A base pair and also directs from C to G for C:G base pair. The PMF can increase the polarity of the DNA base pairs. Whereas the reverse PMF directs from A to T for T:A base pair and also directs from G to C for C:G base pair, and it can decrease the polarity of DNA base pairs.

The effect of PMF on T:A and C:G base pairs was different depending on the nucleotide exposure time (NET), and in order to affect the cyclic PMF from a DNA base pair to the next DNA base pair successively the NET should be less than the T2 relaxation time of a hydrogen bond by 100 Gauss, about 100 msec. However, the real NET for T:A or C:G base pairs is necessary to be directly determined by simple HMR-GR experiment *in vitro*.

For the HMR-GR experiment to determine the most effective NET for each T:A and C:G pair the synthetic oligo-dsDNAs, 10 mM 6(2T2A)•6(2T2A) and 10 mM 6(2C2G)•6(2C2G), were separately prepared in 0.01M NaCl solution, which were composed of T:A and C:G base pairs, respectively. Each oligo-dsDNA was treated with the HMR-GR using different NETs, i.e., 10, 15, 20, 25, 30, 35, 40, 45, 50, 55, 60, 65, 70, 75, 80, 85, 90, and 95 msec for each T:A and C:G base pair, and immediately analyzed by HPLC using a filter column in the mobile phase, 0.01M NaCl at 0.1 mL/min. The areas of oligo-dsDNA peaks were detected by UV<sub>260</sub> absorption, and plotted into a graph.

As the variation of the DNA peak may represent the conformational change of oligo-dsDNA, and the increase of DNA peak is supposed to be the expanded conformation of the objective oligo-dsDNA, implicating the active state of oligo-dsDNA. 6(2T2A)•6(2T2A) composed of T:A base pairs showed the maximum increase

of DNA peak at 50 msec NET, while 6(2C2G)•6(2C2G) composed of C:G base pairs showed the maximum increase of DNA peak at 80 msec NET (Figure 3). Although the most effective NET for T:A or C:G base pair in the different objective DNAs is necessary to be determined by *in vitro* HMR-GR experiment using the relevant objective oligo-dsDNA separately, in the present study the NET was set as 50 msec for T:A base pair and 80 msec for C:G base pair in the targeting the different sequences of oligo-dsDNAs and objective DNA motifs of plasmid DNAs.

**Fig. 3**

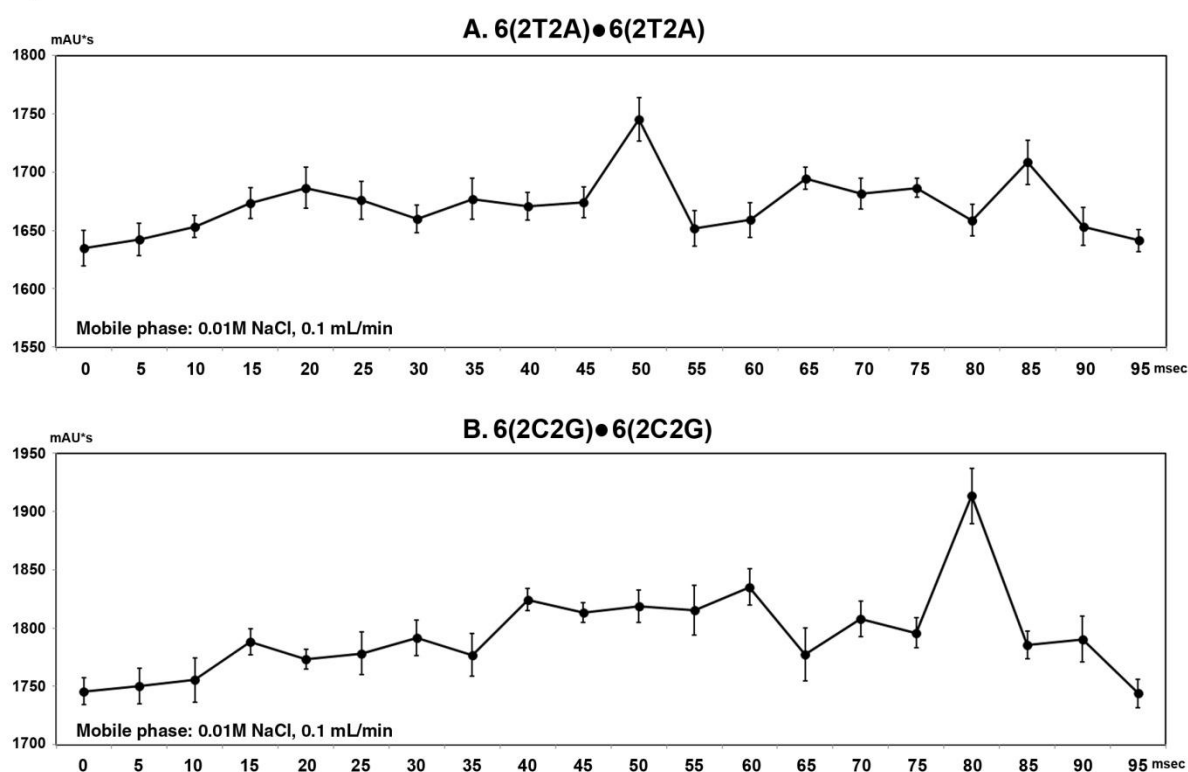


Figure 3. The most effective nucleotide exposure time (NET) of magnetic field is different between T:A and C:G base pairs. 10 mM 6(2T2A)•6(2T2A) and 10 mM 6(2C2G)•6(2C2G) were made by hybridizing the synthetic 6(2T2A) and 6(2C2G) in 0.01M NaCl solution, respectively. These oligo-dsDNAs are in low entropy state and favorable to detect the most effective NET. The 6(2T2A)•6(2T2A) composed of T:A base pairs showed the most increased DNA peak by 50 msec NET, implicating that the T:A base pair was the most effective by 50 msec NET. While the 6(2C2G)•6(2C2G) composed of C:G base pairs showed the most increased DNA peak by 80 msec NET, implicating that the C:G base pair was the most effective by 80 msec NET.



### ***Design of HMR-GR apparatus***

HMR-GR is basically designed to affect objective DNAs that are aligned in one direction, by sequentially simulating the angular differences of DNA base pairs. However, since DNA exists in microscopic scale as a form of nuclear chromosome ultrastructure, it is impossible to align the target DNAs in the same direction. Nevertheless, DNAs are distributed regularly in every direction so 1/4 of the target DNAs can be affected by HMR-GR. This physical efficiency will be discussed later in the next section.

In accordance with the DNA structure, the counter-clockwise PMFs for the sense sequence of objective DNA (Figure 4A,B) is first imposed, immediately followed by the clockwise PMFs for the antisense sequence of objective DNA (Figure 4C,D). The objective DNA is readily activated by the optimal PMF/NET of objective DNA sequence, while other DNAs that have different polarity patterns from objective DNA are not properly activated.

The HMR-GR is most effective to target 20-30 bps, 2-3 turns of DNA duplex, of which hydrogen bonds are placed nearly in the same plane. The HMR-GR apparatus, a horizontal magnetic simulator for DNA duplex is also able to be inclined three-dimensionally to adjust the optimal HMR plane for the objective DNAs.

Although the HMR-GR apparatus elicits the electromagnetic field, the magnetic field is focused and condensed at the central area between a pair of electromagnet arranged longitudinally, while the electric field was mostly dispersed outward from the electromagnet. And more the HMR-GR system has a shielding structure for electric field by nonmagnetic metals to protect the central area between pairs of electromagnet. Therefore, it was presumed that the effect of HMR-GR induced in the central area was mainly originated from the magnetic field.

**Fig. 4**

**Counter-clockwise rotation followed by clockwise rotation for both strands of DNA duplex**

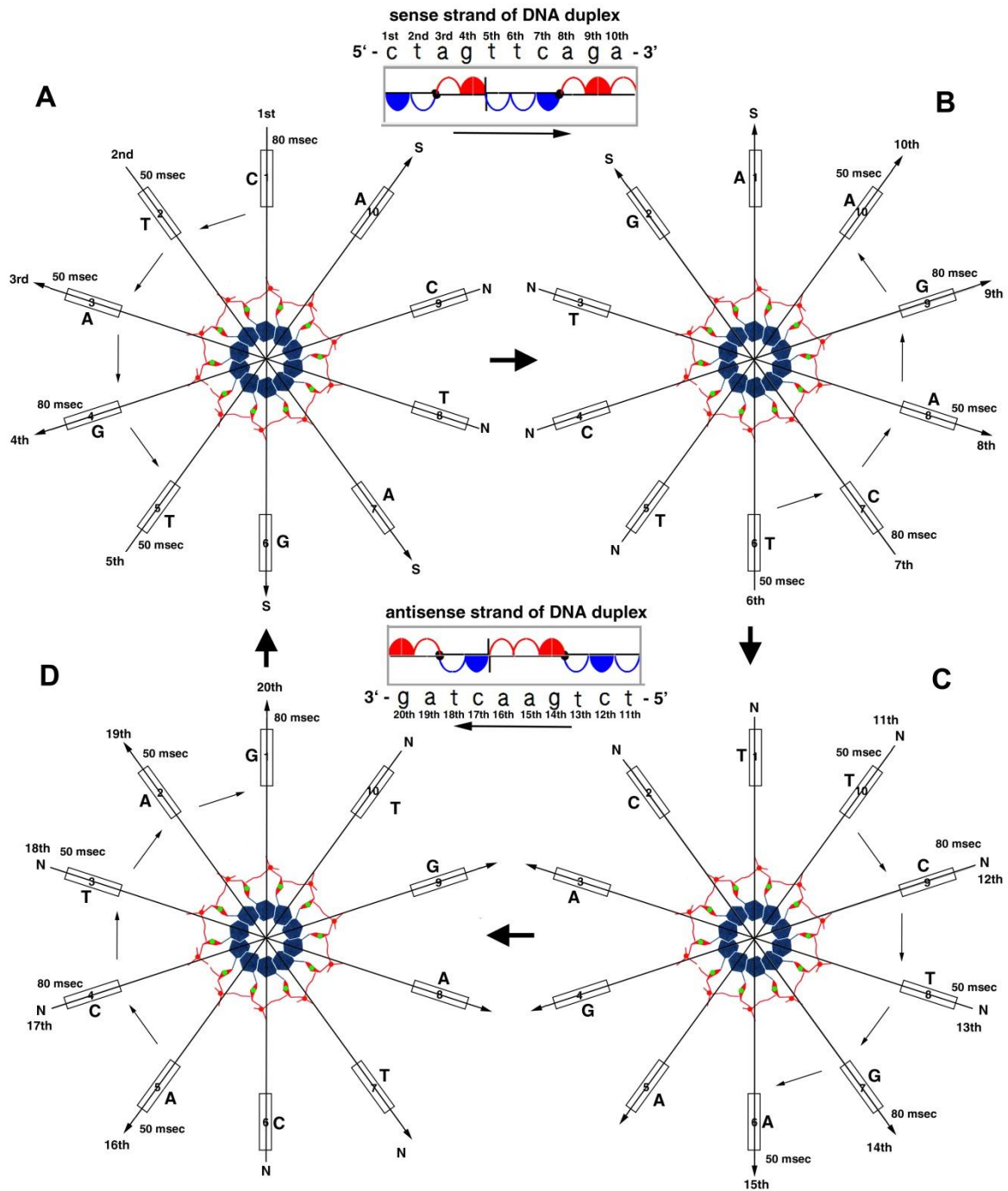


Figure 4. HMR-GR using the DNA sequence of CTAGTTCAGA is shown in the order of (A)-(D). The target DNA is assumed to be laid horizontally so that its DNA orientation heads directly outward from the page. The DNA base pairs are sequentially targeted by PMF, which directs T→A for T:A base pair and C→G for C:G base pair. The NET is set as 50 msec for T:A pair and 80 msec for C:G pair. To simulate both strands of DNA base pairs, HMR-GR is first performed by counter-clockwise PMFs using the sense sequence, immediately followed by clockwise PMFs using the antisense sequence.

### ***Physical efficiency of HMR-GR***

The DNA duplex in Fig 4A (DNA orientation: +z axis direction) whose sense sequence (solid line) heads upward and antisense sequence (dashed line) heads downward, is assumed to be fully affected by HMR-GR. However, such an aligning can hardly happen due to the directional randomness of DNA segments in three dimensions. If the same type of DNA segment is either laid horizontally, or erected vertically but flipped up-side down so that its DNA orientation points  $-z$  axis direction, then it is assumed to have no effect from the same PMFs. In general, the physical efficiency of HMR-GR on a DNA segment is

$$\gamma(\theta, \varphi) = \begin{cases} \cos \varphi, & 0 < \varphi < \pi/2 \\ 0, & \pi/2 \leq \varphi < \pi \end{cases}$$

where  $(\theta, \varphi)$  denotes the direction of its DNA orientation represented in the spherical coordinate system ( $0 \leq \theta < 2\pi$ ,  $0 < \varphi < \pi$ ). Then the average physical efficiency of HMR-GR on randomly distributed DNA duplex can be easily computed as  $1/4$ . (Using the spherical coordinate system,  $(x, y, z) = (r \sin \varphi \cos \theta, r \sin \varphi \sin \theta, r \cos \varphi)$ ,  $0 \leq \theta < 2\pi$ ,  $0 < \varphi < \pi$ ,  $r > 0$ , the average physical efficiency is  $\frac{1}{4\pi r^2} \int_{\theta=0}^{2\pi} \int_{\varphi=0}^{\pi/2} \cos \varphi \cdot r^2 \sin \varphi \, d\varphi \, d\theta = \frac{1}{4}$  ( $r = 1$ )). Therefore, due to the physical randomness of the DNAs in three dimensions, HMR-GR can affect the objective DNAs up to maximum physical efficiency 25%.

**Fig. 5**

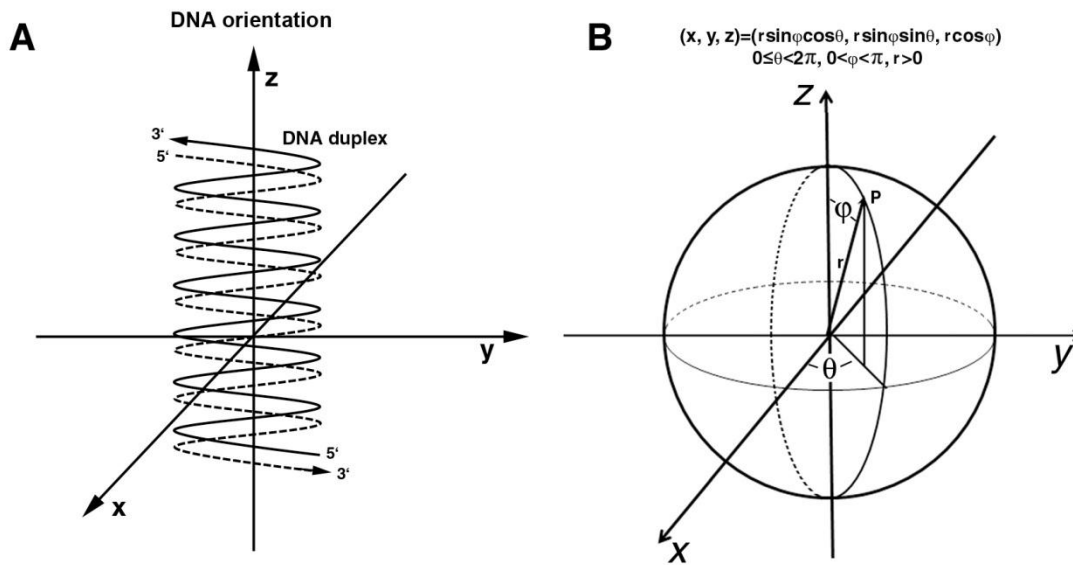


Figure 5. A model for the physical efficiency of HMR-GR on DNAs. (A) A vertically erupted DNA duplex whose sense sequence (solid line) heads upward has physical efficiency 1 with respect to its corresponding PMFs. In this case, its DNA orientation is in the direction of +z axis. If the DNA orientation heads -z axis direction, then its physical efficiency is 0 with respect to the same PMFs. (B) When  $(\theta, \varphi)$  denotes the direction of the DNA orientation in the spherical coordinate system ( $0 \leq \theta < 2\pi, 0 < \varphi < \pi$ ), the physical efficiency of HMR-GR on the DNA duplex is  $\gamma(\theta, \varphi) = \begin{cases} \cos \varphi, & 0 < \varphi < \pi/2 \\ 0, & \pi/2 \leq \varphi < \pi \end{cases}$ . The average physical efficiency of target DNA duplex distributed randomly in three dimensional space is  $\frac{1}{4\pi r^2} \int_{\theta=0}^{2\pi} \int_{\varphi=0}^{\pi/2} \cos \varphi \cdot r^2 \sin \varphi \, d\varphi \, d\theta = \frac{1}{4}$  ( $r = 1$ ).

## MATERIALS AND METHODS

### ***HMR-GR effect on oligo-dsDNAs, 6(2T2A)●6(2T2A) and 6(2C2A)●6(2T2G)***

The *in vitro* hybridized oligo-dsDNA has been denatured by heating, depressed by cooling during annealing procedure, and resulted in the shrunken conformation of dsDNA. We hypothesized that the HMR-GR can renature the oligo-dsDNA, which is remodeled by the polarized electrostatic charge of DNA base pairs, and resulted in the expanded conformation of active dsDNA. The change of DNA conformation is detectable by UV<sub>260</sub> absorption in HPLC analysis.

10mM 6(2T2A)●6(2T2A) and 10mM 6(2C2A)●6(2T2G) were separately dissolved in 0.01M NaCl solution, denatured by heating up to 90°C, and hybridized by slow cooling to room temperature. In the experiment group the oligo-dsDNA, 6(2T2A)●6(2T2A) and 6(2C2A)●6(2T2G), were treated with the HMR-GR using each DNA sequence, while the positive control groups were treated with the HMR-GR using random sequence (6(ACGT)) or poly-A sequence (24A). And the negative control group was done without the HMR-GR. Each 10 μL of DNA sample was injected in every 10 min until 120 min, and analyzed by HPLC at UV<sub>260</sub>.

The HMR-GR effect was observed in the synthetic oligo-dsDNA via their conformational changes. The minute conformational changes of oligo-dsDNA, less than 1%, were detected by the HPLC using only a filter column, which gave no interference of beads, and 0.01M NaCl mobile solution in order to provide the minimum entropy state of dsDNA. Multiple repeated assays for the incremental changes of oligo-dsDNA conformation were plotted into a graph.

### ***Restriction endonuclease (RE) digestion under HMR-GR***

Plasmid DNA (pBluescript SK(-), Y166) inserted with rat amelogenin cDNA (NM\_019154) was digested with each DNA restriction enzyme under HMR-GR using each RE site sequence. For example, 5μg of Y166 was digested with 5U XhoI enzyme under the HMR-GR using an XhoI site sequence, CTCGAG, at room temperature, 23°C. The RE digestion treated with the HMR-GR using a random sequence, ACGTAC, or done without HMR-GR was simultaneously performed as the positive or the negative control in the same condition, respectively. The DNA product after XhoI digestion for 60 min was electrophoresed in 1% agarose gel, stained with ethidium bromide (EtBr, 0.1μg/mL) for 10 min, and detected under UV illumination. On the other hand,

the DNA product was also prestained with EtBr (1  $\mu\text{g}/\text{mL}$ ) for 1 min, electrophoresed with 1% agarose gel, and detected under UV illumination. The weakly bound EtBr was detached from the DNA during electrophoresis, because the EtBr migrated to the cathode contrary to the DNA.

The RE digestion assay to know the HMR-GR effect on plasmid DNA was performed under strict control of experimental condition and time schedule. The visualization of digested DNA fragments was carried out by the post-electrophoresis EtBr staining as well as pre-electrophoresis EtBr staining, and compared each other to reduce the background staining. And more, because the plasmid DNAs linearized by RE digestion have extended structures to absorb more UV light than the native plasmid DNAs which are in circular and coiled structure, the digested DNA fragments were directly quantitated by HPLC method using non-hydrophobic column of Diol-300 column (YMC, USA) at  $\text{UV}_{260}$ . The mobile phase of HPLC was in 0.1M NaCl at 1.6 mL/min. The incremental data depending on the RE digestion time were plotted into a graph, and compared with each other.

### ***In vitro RNA transcription under HMR-GR***

*In vitro* RNA transcription assay was performed using linearized template DNAs which contained about 500-600 bps of human elafin, VEGF, and vWF genes separately. For the reaction of *in vitro* transcription about 0.8  $\mu\text{g}$  of each template DNA was dissolved in 20  $\mu\text{L}$  transcription buffer (40mM Tris-HCl, pH 8.0, 10mM  $\text{MgCl}_2$ , 10mM DTT, 4mM spermidine, 10 mM NaCl, 50  $\mu\text{g}/\text{mL}$  BSA) with 1 unit/ $\mu\text{L}$  RNase inhibitor, 0.4 units/ $\mu\text{L}$  RNA polymerase, and 0.5mM NTP mixture (USB Corp. Ohio, USA), and incubated at room temperature (23°C) for 20 or 40 min. During the incubation time, each template DNA of elafin, VEGF, or vWF was placed under HMR-GR using T3, T7, and SP6 promoter sequence at room temperature, respectively. After the experiment the mixtures were added with 1 unit of DNase I and incubated for 10 min at 37°C to degrade the template DNA, and immediately electrophoresed using 1% agarose gel and DEPC-based buffer. The RNA products were stained with EtBr and detected under UV illumination.

### ***Green Fluorescence Protein (GFP) production under HMR-GR***

*E. coli* transfected with pE-GFP-1 vector (Clontech, USA) was cultured in LB media containing kanamycin (50  $\mu\text{g}/\text{mL}$ ) in room temperature, about 23°C. The pE-GFP-1 vector had a GFP gene, of which 5'

flanking end was inserted with T3 promoter. The standard *E. coli* culture mixture was prepared in the concentration of 0.5 at OD<sub>600</sub> by measuring with UV-spectrometer. For the HMR-GR experiment 1.5 mL of the standard *E. coli* culture mixture was placed under the HMR-GR using a T3 promoter sequence in room temperature. On the other hand, the standard *E. coli* culture mixture of the positive or negative control group was also incubated under the HMR-GR using a random sequence (6(ACGT)) or without HMR-GR, respectively, in the same procedure of the experimental group. After 3 or 5 hours of the *E. coli* culture with HMR-GR the GFP was subsequently detected by spectrofluorometer (excitation; 488 nm, emission; 507 nm, FP-6500, Jasco, Japan) and analyzed statistically.

### ***β-galactosidase production under HMR-GR***

pBluescript SK(-) vector (Stratagene, USA), which has a LacZ gene with a T3 promoter and a T7 promoter in its 5' and 3' flanking ends, respectively, was transfected into *E. coli*, and cultured in LB media containing ampicillin (100 µg/mL) to prepare the standard *E. coli* culture mixture in the concentration of 0.5 at UV<sub>600</sub>. 1.5 mL of the standard *E. coli* culture mixture was used for each HMR-GR experiment.

The experimental group was incubated under HMR-GR using a T3 promoter sequence in room temperature, while the positive control group was incubated under the HMR-GR using a sense sequence of T7 promoter or antisense sequence of T3 promoter, and the negative control group was incubated without HMR-GR in the same condition.

For the β-galactosidase assay the culture was adjusted to 1 mM IPTG (isopropyl-B-D-thiogalactopyranoside) and 10 mM X-Gal (5-bromo-4-chloro-3-indolyl-β-D-galactoside), and after 12 hours incubation of the experiment the X-Gal reaction was detected at 380 nm by UV-spectrometer and subsequently analyzed statistically.

## **RESULTS**

### ***HMR-GR effect on oligo-dsDNAs, 6(2T2A) ●6(2T2A) and 6(2C2A) ●6(2T2G)***

With the most effective NET of magnetic field, 50 msec for T:A and 80 msec for C:G base pair, *in vitro* experiment was performed to know the conformational change of DNA by the HMR-GR targeting oligo-dsDNAs, 6(2T2A)•6(2T2A) and 6(2C2A)•6(2T2G). The changes of DNA peak areas were detected by HPLC method. The DNA peak areas of both 6(2T2A)•6(2T2A) and 6(2C2A)•6(2T2G) gradually increased by the HMR-GR using the sequence of each oligo-dsDNA until 120 min of the HMR-GR. 6(2C2A)•6(2T2G) was more rapidly increased within 40 min of HMR-GR than 6(2T2A)•6(2T2A) (Figure 6A and B).

On the other hand, the positive control groups treated with the HMR-GR using the sequence of 6(ACGT) showed the fluctuating changes of DNA peaks contrast to the experimental group. Their DNA peaks were irregularly variable in the early stage until 80 min, thereafter became slightly increased. Additional positive control groups treated with the HMR-GR using poly-A sequence of 24A showed gradual decrease of DNA peaks until 120 min of HMR-GR time. The negative control group which was not treated with the HMR-GR showed almost no change of DNA peak during the whole HMR-GR time (Figure 6).



Fig. 6

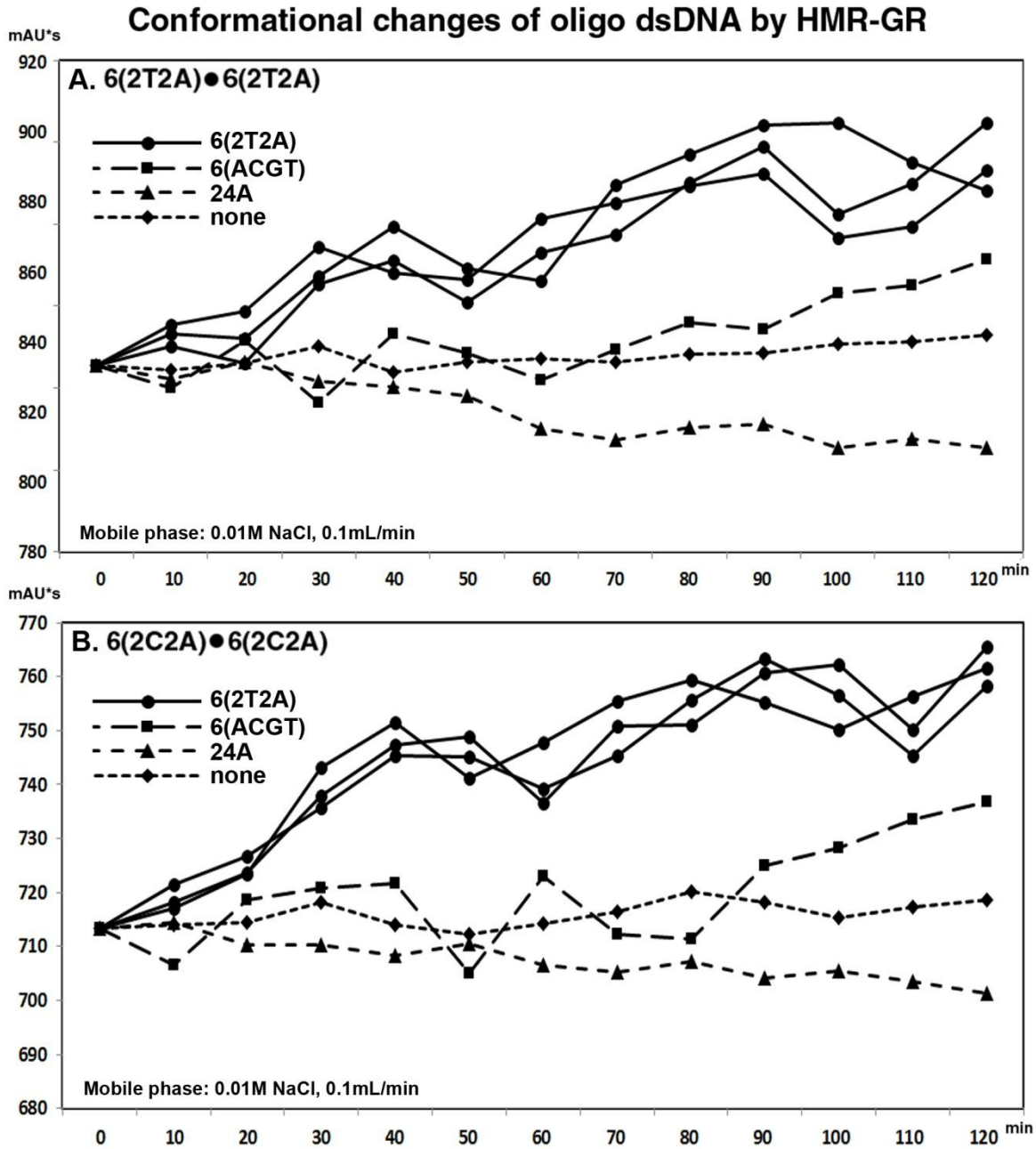


Figure 6. HPLC analysis for the conformational changes of two oligo-dsDNA (A: 6(2T2A)•6(2T2A), B: 6(2C2A)•6(2T2G)) by the HMR-GR. Comparison of HPLC-measured DNA peaks among the representative three experiment groups treated with HMR-GR using the sequences of each oligo-dsDNA, the positive control groups treated with HMR-GR using a random sequence (6(ACGT)) or poly-A sequence (24A), and the negative control group done without the HMR-GR. The experiment groups showed the gradual increase of DNA peaks until 120 min, which were comparable to those of the positive and negative control groups. However, 6(2C2A)•6(2T2G) was slightly more responsive by the HMR-GR than 6(2T2A)•6(2T2A).

### ***Restriction endonuclease (RE) digestion under HMR-GR***

The RE digestion assay was performed under HMR-GR to know the specific effect of the HMR-GR using only 6 bps sequence of each RE binding site. In the electrophoresis analysis of the digested plasmid DNA the experiment group treated with the HMR-GR using an XhoI site sequence, CTCGAG, showed more XhoI digestion of Y166 DNA than the positive or negative control group treated with the HMR-GR using a random sequence (ACGTAC) or done without HMR-GR, respectively. The experimental group showed more digestion of plasmid DNA than the positive and negative control groups, and these results became contrast in the pre-electrophoresis EtBr staining compared to in the post-electrophoresis EtBr staining, because the nonspecific bindings of EtBr were gradually removed during the electrophoresis (Figure 7).

In the HPLC analysis for the digested DNA the experiment group treated with the HMR-GR using an XhoI or a BamHI site sequence, CTCGAG or GGATCC, respectively, produced greater DNA peaks in the time dependent manner than the positive and negative control groups treated with HMR-GR using a random sequence of ACGTAC and done without HMR-GR, respectively. The experiment groups showed the greater incremental line during the incubation time until 100 min compared to the positive and negative control groups as shown in Figure 7. The RE digestion under the HMR-GR using each RE site sequence was rapidly enhanced in 10-60 min compared to the positive and negative control groups, and thereafter it became plateau until 100 min (Figure 8A and B).

**Fig. 7**

**XhoI digestion of plasmid DNA by HMR-GR**

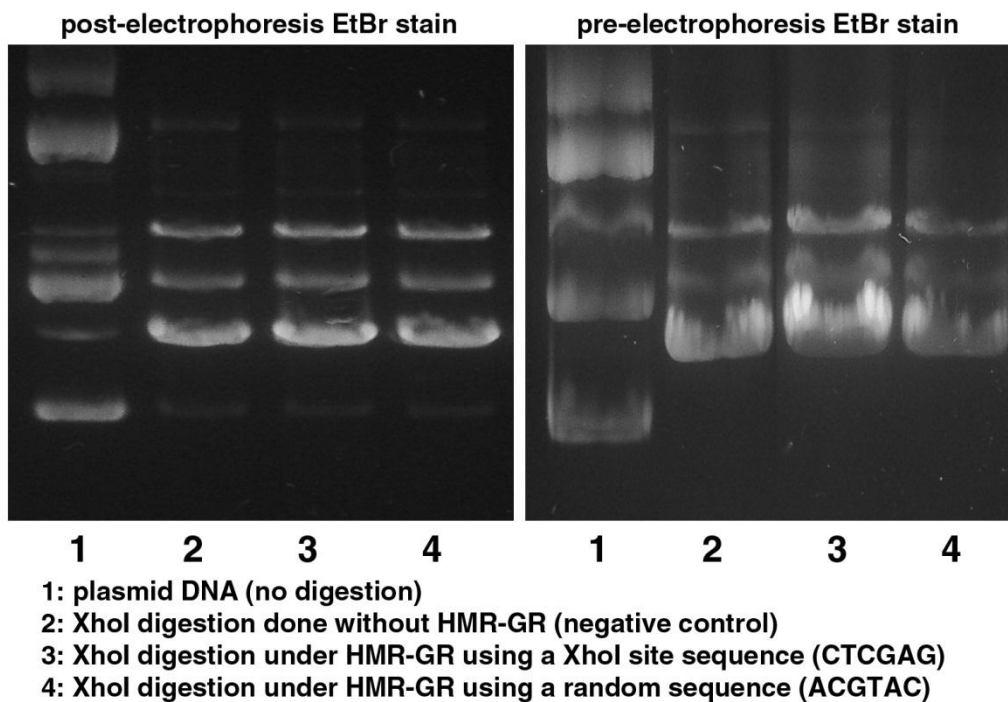
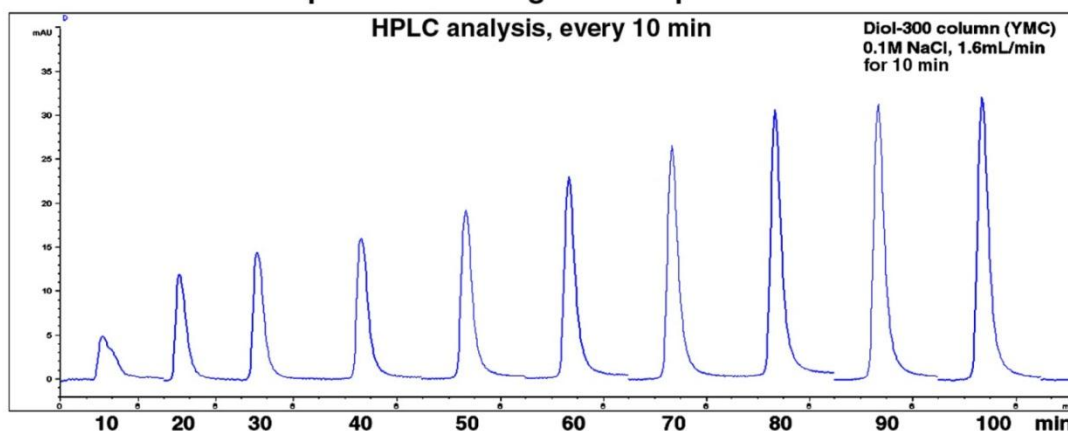


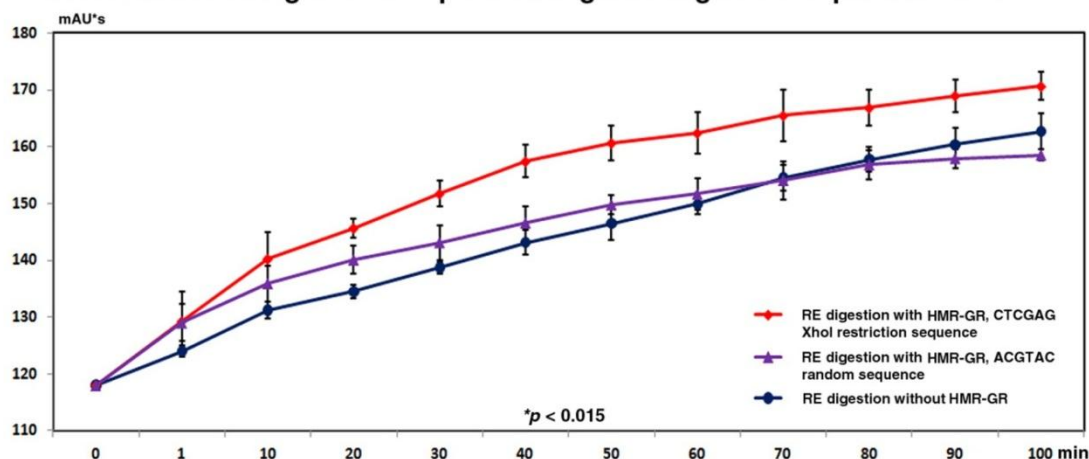
Figure 7. HMR-GR effect on the XhoI digestion of plasmid DNA (Y166). Both in the pre- and post-electrophoresis EtBr stainings, the DNA bands digested by XhoI under the HMR-GR using an XhoI site sequence, CTCGAG, was stronger than those of the positive control treated with the HMR-GR using a random sequence, ACGTAC, and the negative control done without HMR-GR. A representative case was presented from triplicate experiments.

**Fig. 8**

**A. Increase of DNA peak after RE digestion of plasmid DNA until 100 min**



**B. Incremental changes of DNA peak during XhoI digestion of plasmid DNA**



**C. Incremental changes of DNA peak during BamHI digestion of plasmid DNA**

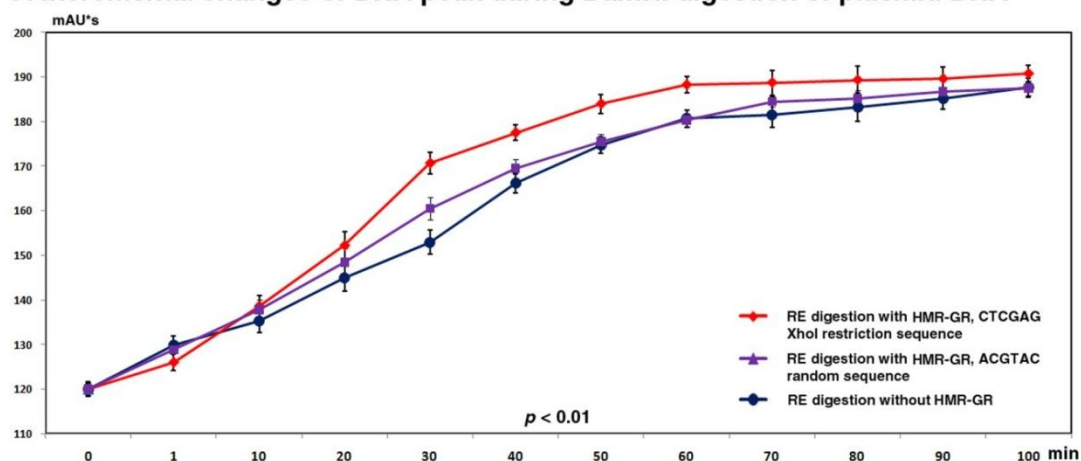


Figure 8. HPLC analysis for the XhoI and BamHI digestions of plasmid DNA (Y166). (A) Standard incremental DNA peak of HPLC analysis in the negative control group. Both the XhoI (B) and BamHI (C) digestions under HMR-GR using a RE site sequence, CTCGAG or GGATCC, respectively, produced greater DNA peak than the RE digestion treated with HMR-GR using a random sequence, ACGTAC, or done without HMR-GR.

\*Significant differences among the groups (B:  $p < 0.015$ , C:  $p < 0.01$ ) was seen by one-way analysis of variant (ANOVA, SPSS version 18.0 software) followed by Scheff's test.

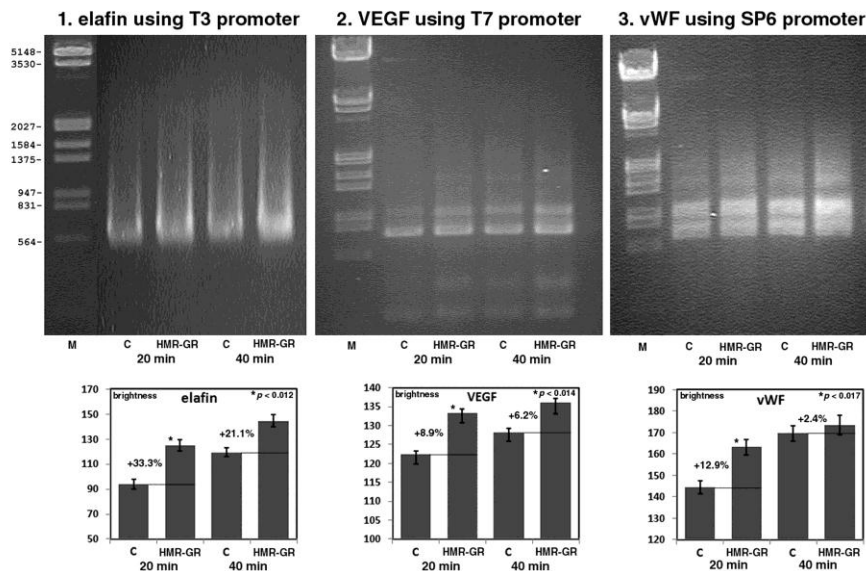
## *In vitro* RNA transcription under HMR-GR

The *in vitro* RNA transcriptions of elafin, VEGF, and vWF under the HMR-GR showed more RNA production than the control group done without HMR-GR. The experiment group treated with the HMR-GR showed more production of RNA in 20 min of transcription than the control group, and continuously maintained the increased RNA production in 40 min of transcription (Figure 9A). Although the *in vitro* RNA transcription assay had a limitation due to the rapid degradation of RNA, the immediate electrophoresis using RNAase protective agarose gel after each experiment clearly showed the contrast level of RNA production, which was more abundant in the experiment group than the control group in the time dependent manner.

On the other hand, the experiment to compare the RNA transcription effect of HMR-GR using the PMF or the reverse PMF of T3 promoter sequence disclosed that the elafin HMR-GR using the PMF of T3 promoter sequence produced more RNA production than the elafin HMR-GR using the reverse PMF of T3 promoter sequence. And more, the elafin RNA production by using the reverse PMF of T3 promoter sequence was slightly reduced in comparison with that of the negative control done without the HMR-GR (Figure 9B).

**Fig. 9**

**A. *in vitro* RNA transcription of human elafin, VEGF, and vWF DNA under HMR-GR using the sequence of T3, T7, and SP6 promoter, respectively**



**B. *in vitro* RNA transcription under HMR-GR using the PMF or reverse PMF of T3 promoter sequence.**

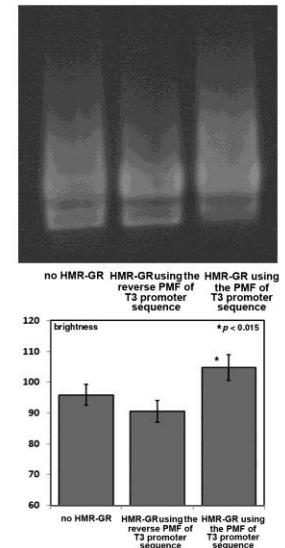


Figure 9. *In vitro* RNA transcription of human elafin, VEGF, and vWF DNAs under HMR-GR using a sequence of T3, T7, or SP6 promoter, respectively, and analyzed by densitometer. (A) The *in vitro* RNA transcriptions of elafin, VEGF, and vWF under the HMR-GR produced more RNA than those done without HMR-GR (A1-A3). (B) *In vitro* RNA transcription of elafin DNA under HMR-GR using the PMF or the reverse PMF of T3 promoter sequence. The HMR-GR using the PMF of T3 promoter sequence produced more RNA transcription than the HMR-GR using the reverse PMF of T3 promoter sequence.

\*Significant differences among the groups (A1:  $p < 0.012$ , A2:  $p < 0.014$ , A3:  $p < 0.017$ , B:  $p < 0.015$ ) was seen in

the proportionated data from multiple repeated experiments.

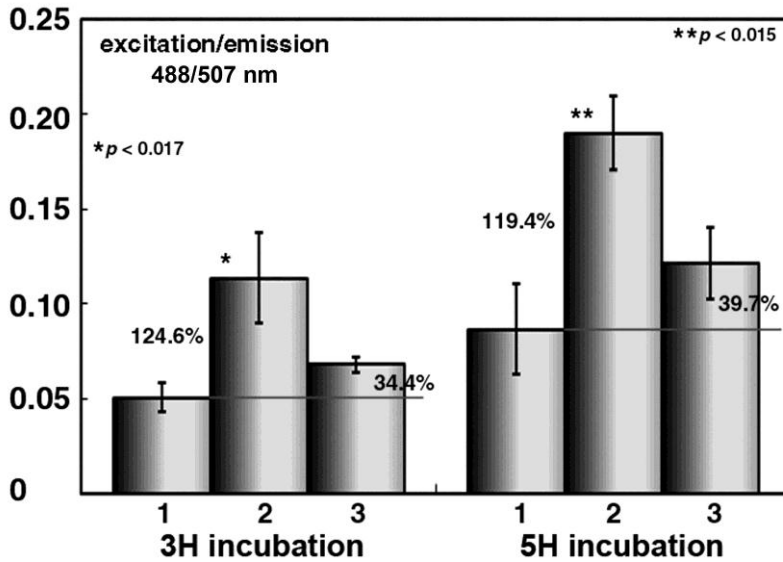
### ***Green Fluorescence Protein (GFP) production under HMR-GR***

The HMR-GR effect on the pE-GFP-1 vector transfected into *E. coli* was directly evaluated by detecting the GFP production using spectrofluorometer. The experiment group treated with HMR-GR using a T3 promoter sequence to target the GFP gene in pE-GFP-1 vector produced more GFP than the positive and negative control groups consistently until 5 hours of the experiment (Figure 10).

The GFP production under the HMR-GR using a T3 promoter sequence significantly increased by about 124.6% and 119.4% compared to the negative control done without the HMR-GR in 3 hours and 5 hours of the experiment, respectively, while the GFP production under the HMR-GR using a random sequence (6(ACGT)) increased by about 34.4% and 39.7% compared to the negative control done without the HMR-GR in 3 hours and 5 hours of the experiment, respectively.

**Fig. 10**

#### **Spectrofluorometry for GFP production under HMR-GR**



1: control, without HMR-GR 2: HMR-GR using T3 promoter sequence  
3: HMR-GR using random sequence, 6(ACGT)

Figure 10. Spectrofluorometer analysis for the GFP production from pE-GFP-1 vector under HMR-GR. The experiment group treated with HMR-GR using a T3 promoter sequence produced more GFP than the positive control group treated with HMR-GR using a random sequence, 6(ACGT), as well as than the negative control group done without HMR-GR.

\*Significant differences among the groups ( $p < 0.017$ ) was seen in the proportionated data from multiple repeated experiments.

### ***β-galactosidase production under HMR-GR***

The β-galactosidase assay was performed with *E. coli* transfected with pBluescript SK(-) vector, which contained a LacZ gene with a T3 promoter and a T7 promoter in its 5' and 3' flanking ends, respectively. This experiment provided the variable comparison among the HMR-GRs using a T3 promoter sequence, a T7 promoter sequence, or an antisense sequence of T3 promoter.

Resultantly, the experiment group treated with the HMR-GR using a T3 promoter sequence showed stronger X-Gal reaction compared to the HMR-GRs using a T7 promoter sequence or an antisense sequence of T3 promoter. The 12 hours of the HMR-GR using a T3 promoter sequence showed stronger X-Gal reaction than the negative control by about 6.5% increase, while the HMR-GRs using a T7 promoter sequence or an antisense sequence of T3 promoter showed stronger X-Gal reaction than the negative control by about 2.8% or 1.9% increase, respectively (Figure 11).

**Fig. 11**

### **β-galactosidase production under HMR-GR**

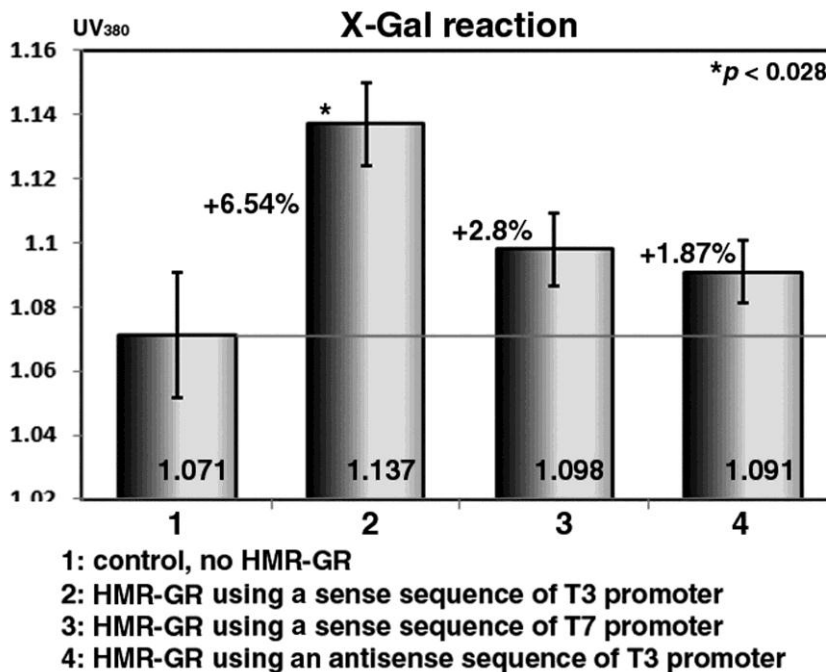


Figure 11. The *E. coli* culture for LacZ gene expression under HMR-GR. The experiment group treated with HMR-GR using a T3 promoter sequence showed more X-Gal reaction than the positive control groups treated with HMR-GR using a T7 promoter sequence or an antisense sequence of T3 promoter, as well as than the negative control group done without HMR-GR. \*Significant differences among the groups ( $p < 0.028$ ) was seen in the proportionated data from multiple repeated experiments.

## DISCUSSION

HMR-GR has been developed to overcome many difficult problems in bio-medical science by targeting DNA duplex directly through the HMR-GR which is almost absent of biohazards. The HMR-GR is one of different gene therapy methods investigated widely, however, the HMR-GR experiments presented in this study are the representative models to activate oligo-dsDNA directly, and to control the expressions of objective genes by activating the RE binding site sequences or promoter sequences by the HMR-GR.

### ***HMR-GR effect on oligo-dsDNAs, 6(2C2A)•6(2T2G) and 6(2T2A)•6(2T2A)***

The DNA duplexes targeted by HMR-GR are supposed to have different hybridization status depending on their DNA base pair polarities, and resulted in their conformational changes. If the HMR-GR increases the hybridization energy of target DNA duplex by the specific PMF corresponding to the oligo-dsDNA, the target DNA duplex will be activated and transformed to the expanded conformation. The experiment of HMR-GR effect on oligo-dsDNAs is to observe the direct response of oligo-dsDNAs by the electrostatic activation of HMR. As the conformational change induced by the HMR-GR is essential to the function of target DNA, the *in vitro* HMR-GR assay of oligo-dsDNA was measured by HPLC analysis using only a simple filter column to prevent the experimental errors caused by the non-specific DNA binding to column beads.

Particularly, the oligo-dsDNAs, 6(2T2A)•6(2T2A) and 6(2C2A)•6(2T2G), were prepared by chemical synthesis and hybridization in 0.01M NaCl solution, which can provide the minimum entropy state of oligo-dsDNA (17-19). 6(2T2A)•6(2T2A) is composed of T:A base pairs, and 6(2C2A)•6(2T2G) has no secondary structure. However, according to the potential of DNA base pair polarity the 6(2C2A)•6(2T2G) has stronger hybridization energy than the 6(2T2A)•6(2T2A). Finally, both 6(2T2A)•6(2T2A) and 6(2C2A)•6(2T2G) treated with the HMR-GR using the PMFs corresponding sequence to each oligo-dsDNA showed the gradual increase of DNA peak in HPLC until 120 min, while the positive control groups treated with HMR-GR using a random sequence (6(ACGT)) or a poly-A sequence (24A) showed irregularly fluctuating changes of oligo-dsDNA peaks, and the negative control group done without HMR-GR were almost not changed until 120 min of experiment. And in comparison of HMR-GR responsibility between 6(2T2A)•6(2T2A) and 6(2C2A)•6(2T2G) the 6(2C2A)•6(2T2G) showed greater incremental slope than the 6(2T2A)•6(2T2A) within 40 min of HMR-



GR time.

Although it is not easy to detect the conformational changes of DNA duplex in buffer solution, and the precise detection of transient change of DNA conformation induced by the HMR-GR is almost impossible even though the recent advance of molecular biological techniques (20,21), the HPLC analysis used in this study to detect the conformational changes of oligo-dsDNA was consistently applicable for every DNA sample obtained from the HMR-GR experiments. It gave fairly accurate information about the conformational changes of oligo-dsDNA, which was less than 1% change of DNA conformation. However, the increase of DNA peak by the HMR-GR may directly indicate the swelling of DNA conformation. This increase of DNA peak was conspicuous in the HMR-GR using the sequence of objective DNA but not in the HMR-GR using a random sequence (6(ACGT)) or a poly-A sequence (24A). Therefore, it is presumed that the HMR-GR using the objective DNA sequence can change the objective DNA into a swollen conformation, which is usually found in the activated DNAs (22-24).

### ***Restriction endonuclease (RE) digestion under HMR-GR***

In the molecular event of RE digestion the initial step of RE digestion may require the binding of RE enzyme to the specific sequence of RE binding site. The RE binding site sequence of objective DNA should be activated and expanded to adapt the RE binding properly (25). This RE digestion experiment under HMR-GR was to know the specific activation of target DNA composed of only six base pairs by the HMR-GR. However, the HMR-GR using the relevant RE site sequence more enhanced the RE digestion than the positive control group performed under HMR-GR using a random sequence, ACGTAC, as well as the negative control group performed without the HMR-GR.

In the present study the RE-digested products of plasmid DNA were analyzed by both electrophoresis and HPLC methods. The post-electrophoresis EtBr staining method which was commonly done to detect the DNA fragment was not appropriate to observe the precise amount of DNA fragment due to the non-specific binding of EtBr, which became gradually condensed depending on the time of staining. Therefore, the pre-electrophoresis EtBr staining method was applied to compare the amount of DNA fragment with each other. In the case of the pre-electrophoresis EtBr staining the non-specific binding of EtBr could be removed during the electrophoresis, thereby the amount of DNA fragment was clearly defined in the gel. But the migration of DNA fragment was markedly interfered and retarded, resulted in the abnormal band shape. However, resultantly the experiment

group treated with HMR-GR using an XhoI site sequence showed more XhoI digestion of Y166 DNA than the positive or negative control group treated with HMR-GR using a random sequence and done without HMR-GR, respectively, both in the observations of pre- and post-electrophoresis EtBr stainings.

Because the UV detection of EtBr staining through the electrophoresis was somehow non-quantitative and incredible to determine the important results of the HMR-GR, the quantitative analysis of the digested DNA fragments was performed with HPLC analysis using non-hydrophobic column, Diol-300. Because the linearized plasmid DNA by RE digestion can absorb more UV<sub>260</sub> light than the super-coiled native plasmid DNA, the DNA peak area separated by the HPLC may imply the relative amount of digested DNA fragment and is comparable with each other. Resultantly, the experiment group treated with the HMR-GR using an XhoI or a BamHI site sequence, CTCGAG or GGATCC, respectively, produced greater DNA peak area than the positive and negative control groups treated with HMR-GR using a random sequence of ACGTAC or done without HMR-GR, respectively. The RE digestion under HMR-GR using a RE site sequence was rapidly enhanced during 10-60 min of experiment compared to the positive and negative control groups, and showed the steep incremental growth curve comparable to those of the positive and negative control groups. Therefore, it is assumed that the HMR-GR using the RE site sequence can activate the RE site sequence of objective DNA, and eventually enhance the DNA digestion by relevant RE enzyme.

Besides the XhoI and BamHI digestions we have examined other different RE digestions using EcoRI, KpnI, PstI, SacI, and XbaI enzymes, and all the RE digestions under HMR-GR using each RE site sequence consistently produced more linearized DNAs than the relevant positive and negative control groups.

### ***In vitro RNA transcription under HMR-GR***

The *in vitro* RNA transcription assay was performed to know the HMR-GR effect on the gene transcription by the HMR-induced activation of relevant promoter sequence. This experiment is the simplest method to identify the effect of HMR-GR whether the relevant gene transcription was enhanced or reduced, but needed to be protected from the degradation of RNA products. As the HMR-GR has a potential to activate specific DNA motifs including promoter sequences as well as RE site sequences, this experiment is an important model to define the HMR-GR-induced regulation of objective gene transcription.

The *in vitro* RNA transcription assay had to be performed in the HMR-GR apparatus, thereby the incubation of RNA transcription mixture was done in the RNase free space of HMR-GR apparatus at room

temperature (23°C), and after the experiment the samples were immediately electrophoresed using RNase-protection agarose gel. In the *in vitro* RNA transcriptions of elafin, VEGF, and vWF the experiment groups treated with the HMR-GR showed more RNA production than the control group done without HMR-GR. The experiment group showed rapid increase of RNA production during the early 20 min and consistently maintained until 40 min. The increase of the HMR-induced RNA transcription may be ascribed to the activated promoters by the HMR-GR, which are subsequently bound more RNA polymerases than the control. However, further study should be followed to identify the precise mechanism of HMR-induce RNA transcription.

The *in vitro* RNA transcription assay is relatively specific to the stimulation of HMR-GR, because no other molecules can mediate the RNA production except the prepared molecules in the RNA transcription mixture. In the comparison between the HMR-GR using PMF and reverse PMF the elafin HMR-GR using the PMF of T3 promoter sequence produced more RNA than the elafin HMR-GR using the reverse PMF of T3 promoter sequence. And the elafin HMR-GR using the reverse PMF of T3 promoter sequence produced less amount of RNA than the negative control done without the HMR-GR. These results may indicate that the HMR-GR using the reverse PMF of objective DNA sequence could inactivate the objective DNA.

The promoter DNA sequences are usually composed of characteristic base pair polarities, which are easily distinguishable from other motif sequences, thus only the specific transcription factor can recognize the promoter region through the molecular interaction (26,27). From the above experiment, it is assumed that the HMR-GR is able to enhance the RNA production by the direct activation of relevant promoter DNA.

### ***Green Fluorescence Protein (GFP) production under HMR-GR***

The GFP reporter protein from pE-GFP-1 vector is able to be directly detected by the spectrofluorometer, thereby the *de novo* production of GFP from the vector can be evaluated to know the expression level of GFP gene. The culture of *E. coli* transfected with pE-GFP-1 vector was performed under the HMR-GR using the T3 promoter sequence for GFP gene transcription. And then the HMR-GR effect on the *de novo* production of GFP was dramatically increased in comparison with those of the positive and negative control groups cultured under the HMR-GR using a random sequence and done without the HMR-GR, respectively.

The experiment group treated with the HMR-GR using a T3 promoter sequence to target the GFP gene in pE-GFP-1vector produced more GFP than the positive and negative control groups consistently until 5 hours of the experiment. In detail, the GFP production under the HMR-GR using a T3 promoter sequence significantly

increased by about 124.6% and 119.4% compared to the negative control done without the HMR-GR in 3 hours and 5 hours of the experiment, respectively, while the GFP production under the HMR-GR using a random sequence increased by about 34.4% and 39.7% compared to the negative control done without the HMR-GR in 3 hours and 5 hours of the experiment, respectively.

These findings of continuous increase of GFP level by the HMR-GR treatment during the experiment period may indicate that the HMR-GR-induced activation of target DNA can be maintained continuously. And more, contrary to the above HMR-GR experiments performed with the synthetic oligo-dsDNAs or linearized plasmid DNAs, the GFP expression experiment was performed with the supercoiled plasmid DNAs in *E. coli*. Therefore, this *in vivo* experiment may significantly imply that the HMR-GR is also able to affect the native genes working in the cells.

### ***β-galactosidase production under HMR-GR***

The β-galactosidase assay using LacZ gene-containing vector is one of the most popular gene regulation experiments, which is unique and easy to do. And more, LacZ gene-containing vectors were well developed to be inserted by both T3 and T7 promoter at 5' and 3' flanking ends of LacZ gene, i.e., pBluescript SK(-) vector. In this study the β-galactosidase expression from the LacZ gene of pBluescript vector was examined in the treatment of the HMR-GR using T3 or T7 promoter sequences. The amount of β-galactosidase production was visualized by chemical reaction of X-Gal, and the blue color of X-Gal was detected by UV-spectrometer at 380 nm. Therefore, the results of the β-galactosidase assay might have a big range of error, but it is still helpful to determine whether the HMR-GR can control the LacZ gene positively or negatively.

Resultantly, the experiment group treated with the HMR-GR using a T3 promoter sequence consistently showed higher X-Gal reaction compared to the positive control group treated with the HMR-GR using T7 promoter sequence and the negative control group done without the HMR-GR. These findings may imply that the HMR-GR can target the specific motif sequences of T3 and T7 promoters, which have quite different Pyu DNA segments each other.

HMR-GR is a novel modality to control the expression of objective gene. Using the different polarities between pyrimidine and purine in DNA base pairs and the different hybridization strength between the T:A and C:G base pairs, The DNA duplex can be targeted by the specific PMF and optimal NET of HMR-GR method. In

this study, the oligo-dsDNA treated with HMR-GR showed the increase of UV<sub>260</sub> absorption which might imply the expanded conformation of active dsDNA. It is also demonstrated that the repeated activation of specific DNA sequences (including the RE site sequences, T3, T7, and SP6 promoter sequences, and different motif sequences of objective DNA) by the HMR-GR enhanced the relevant events of RE digestions, *in vitro* RNA transcriptions, and protein productions from DNA vectors, respectively.

Contrast to other gene therapy methods the HMR-GR can directly target multiple genes sequentially to enhance specific cellular events without using any drug injection and surgical manipulations, and its targeting can be not only available to the whole body but also localized at a tiny area as small as in the microscopic level depending on the scale of HMR-GR apparatus. Therefore, it is suggested that HMR-GR is a reliable method for the gene regulation, which can be applied to treat most of objective tissues safely.

Besides the presented HMR-GR results, we have performed many other HMR-GR experiments on mammalian cell cultures, animal breedings, and vegetable cultivations, etc., which consistently showed significant increase of objective gene expressions as well by the HMR-GR. This HMR-GR method offers a new field of gene regulation that can target all kinds of genes collected in GenBank, therefore, further investigation should be followed in different aspects under world-wide cooperation. The quantum mechanical explanation of HMR-GR in this study is still hypothetical and requires more fundamental experiments in atomic level. And although the concept of DNA base pair polarity was helpful to predict the electrostatic HMR energy, it also neglected to determine the real transient change of electrostatic charge in DNA base pairs. However, the HMR-GR which can specifically activate the DNA motif sequences must be an important gene regulation method to do the more things impossible so far.

## REFERENCES

1. Kim, Y.S., Lee, D.S., Lee, D.G., Lee, S.K., Choi, S.J., Song, I.S., Lee, S.S., Lee, Y.J., Lee, Y.W., Park, S.C. *et al.* (2009) Genetic code is composed of pyrimidine-purine DNA segments as a basic unit displaying DNA base pair polarity. *Medical Hypothesis and Research*, **5**, 1-18.
2. Alia, A., Wawrzyniak, P.K., Janssen, G.J., Buda, F., Matysik, J. and de Groot, H.J. (2009) Differential charge polarization of axial histidines in bacterial reaction centers balances the asymmetry of the special pair. *J Am Chem Soc*, **131**, 9626-9627.

3. Canet, D., Bouguet-Bonnet, S., Aroulanda, C. and Reineri, F. (2007) About long-lived nuclear spin states involved in para-hydrogenated molecules. *J Am Chem Soc*, **129**, 1445-1449.
4. Kuhn, L.T., Bommerich, U. and Bargon, J. (2006) Transfer of parahydrogen-induced hyperpolarization to <sup>19</sup>F. *J Phys Chem A*, **110**, 3521-3526.
5. Jeon, S.I., Kim, D.R. and Lee, S.K. (2001) Changes of Solubility Speed of Salts in Magnetized Water and Crystal Patterns of NaCl, KCl and Gypsum Intermediated by Magnetized Water. *J of the Korean Chemical Society*, **45**, 116-130.
6. Jeon, S.I., Kim, D.R., Lee, S.H., Kim, D.S. and Lee, S.K. (2002) Study on the effect of magnetized water in the precipitation of salts and in the hydration hardening speed of Gypsum Plaster. *The Korean Chemical Society*, **46**, 7-13.
7. Hartwig, S., Voigt, J., Scheer, H.J., Albrecht, H.H., Burghoff, M. and Trahms, L. (2011) Nuclear magnetic relaxation in water revisited. *J Chem Phys*, **135**, 054201.
8. Lane, A.N. (1991) Solution conformation and dynamics of the octadeoxy-nucleotide d(CACTAGTG)<sub>2</sub>: a multinuclear n.m.r. relaxation study. *Carbohydr Res*, **221**, 123-144.
9. Jacobson, J.I. (1991) A look at the possible mechanism and potential of magneto therapy. *J Theor Biol*, **149**, 97-119.
10. Ren, Q., Lu, J., Tan, H.H., Wu, S., Sun, L., Zhou, W., Xie, W., Sun, Z., Zhu, Y., Jagadish, C. *et al.* (2012) Spin-resolved Purcell effect in a quantum dot microcavity system. *Nano letters*, **12**, 3455-3459.
11. Sottini, S. and Groenen, E.J. (2012) A comment on the pseudo-nuclear Zeeman effect. *J Magn Reson*, **218**, 11-15.
12. Lee, S.K. (2001) Selection of PCR primer sequence by the properties of DNA base pair polarity concept. *Korean J of Oral & Maxillofacial Pathology*, **25**, 185-201.
13. Keith, R.F. and Michael, J.W. (1987) Footprinting at low temperatures: evidence that ethidium and other simple intercalators can discriminate between different nucleotide sequences. *Nucl. Acids Res*, **15**, 491-507.
14. Thomas, R.K. and Christian, G.R. (1975) Evidence for sequence preferences in the intercalative binding of ethidium bromide to dinucleoside monophosphates. *J Mol Biol*, **97**, 133-162.
15. Kim, Y.S. and Lee, S.K. (2010) Properties of Extremely Low Frequency Electromagnetic Field and their Effects on Mouse Testicular Germ Cells. *International Journal of Oral Biology*, **35**, 137-144.

16. Shin, H.S., Lee, J.Y., Lee, S.K., Park, S.C. and Chi, J.G. (2000) Pulsating Magnetic Field Effects on in vitro Culture of Human Osteogenic Sarcoma Cells. *The Korean J of Pathology*, **34**, 169-180.
17. Pascal, T.A., Goddard, W.A., 3rd, Maiti, P.K. and Vaidehi, N. (2012) Role of Specific Cations and Water Entropy on the Stability of Branched DNA Motif Structures. *J Phys Chem B*.
18. Ramakrishnan, V., D'Costa, M., Ganesh, K.N. and Sastry, M. (2004) Effect of salt on the hybridization of DNA by sequential immobilization of oligonucleotides at the air-water interface in the presence of ODA/DOTAP monolayers. *J Colloid Interface Sci*, **276**, 77-84.
19. Zinchenko, A.A. and Yoshikawa, K. (2005) Na<sup>+</sup> shows a markedly higher potential than K<sup>+</sup> in DNA compaction in a crowded environment. *Biophys J*, **88**, 4118-4123.
20. Buzio, R., Repetto, L., Giacomelli, F., Ravazzolo, R. and Valbusa, U. (2012) Label-free, atomic force microscopy-based mapping of DNA intrinsic curvature for the nanoscale comparative analysis of bent duplexes. *Nucleic Acids Res*, **40**, e84.
21. Ogasawara, D., Hachiya, N.S., Kaneko, K., Sode, K. and Ikebukuro, K. (2009) Detection system based on the conformational change in an aptamer and its application to simple bound/free separation. *Biosensors & bioelectronics*, **24**, 1372-1376.
22. Claverie-Martin, F. and Magasanik, B. (1992) Positive and negative effects of DNA bending on activation of transcription from a distant site. *J Mol Biol*, **227**, 996-1008.
23. Perez-Martin, J. and Espinosa, M. (1994) Correlation between DNA bending and transcriptional activation at a plasmid promoter. *J Mol Biol*, **241**, 7-17.
24. Rhee, K.Y., Senear, D.F. and Hatfield, G.W. (1998) Activation of gene expression by a ligand-induced conformational change of a protein-DNA complex. *J Biol Chem*, **273**, 11257-11266.
25. Seidel, R., van Noort, J., van der Scheer, C., Bloom, J.G., Dekker, N.H., Dutta, C.F., Blundell, A., Robinson, T., Firman, K. and Dekker, C. (2004) Real-time observation of DNA translocation by the type I restriction modification enzyme EcoR124I. *Nature structural & molecular biology*, **11**, 838-843.
26. Bertram, M.J. and Pereira-Smith, O.M. (2001) Conservation of the MORF4 related gene family: identification of a new chromo domain subfamily and novel protein motif. *Gene*, **266**, 111-121.
27. Fang, B., Mane-Padros, D., Bolotin, E., Jiang, T. and Sladek, F.M. (2012) Identification of a binding motif specific to HNF4 by comparative analysis of multiple nuclear receptors. *Nucleic Acids Res*, **40**, 5343-5356.